21 Apr 2019

Mass Accommodation at a High-Velocity Water Liquid-Vapor Interface

J. Nie

A. Chandra

Z. Liang
Missouri University of Science and Technology, zlch5@mst.edu

P. Keblinski

Recommended Citation

J. Nie et al., "Mass Accommodation at a High-Velocity Water Liquid-Vapor Interface," *Journal of Chemical Physics*, vol. 150, no. 15, article no. 154705, American Institute of Physics, Apr 2019.
The definitive version is available at https://doi.org/10.1063/1.5091724

The Journal of Chemical Physics

Mass accommodation at a high-velocity water liquid-vapor interface

Cite as: J. Chem. Phys. **150**, 154705 (2019); https://doi.org/10.1063/1.5091724
Submitted: 05 February 2019 • Accepted: 05 March 2019 • Published Online: 17 April 2019

J. Nie, A. Chandra, Z. Liang, et al.

The Journal of Chemical Physics ARTICLE scitation.org/journal/jcp

Mass accommodation at a high-velocity water liquid-vapor interface

Cite as: J. Chem. Phys. 150, 154705 (2019); doi: 10.1063/1.5091724
Submitted: 5 February 2019 • Accepted: 5 March 2019 •
Published Online: 17 April 2019

J. Nie,[1] A. Chandra,[2] Z. Liang,[3] and P. Keblinski[1,a)]

AFFILIATIONS

[1]Department of Materials Science and Engineering, Rensselaer Polytechnic Institute, Troy, New York 12180, USA
[2]Department of Mechanical, Aeronautical and Nuclear Engineering, Rensselaer Polytechnic Institute, Troy, New York 12180, USA
[3]Department of Mechanical Engineering, California State University, Fresno, California 93740, USA

[a)]**Author to whom correspondence should be addressed:** keblip@rpi.edu

ABSTRACT

We use molecular dynamics to determine the mass accommodation coefficient (MAC) of water vapor molecules colliding with a rapidly moving liquid-vapor interface. This interface mimics those present in collapsing vapor bubbles that are characterized by large interfacial velocities. We find that at room temperature, the MAC is generally close to unity, and even with interfaces moving at 10 km/s velocity, it has a large value of 0.79. Using a simplified atomistic fluid model, we explore the consequences of vapor molecule interfacial collision rules on pressure, temperature, and density of a vapor subjected to an incoming high-velocity liquid-vapor interface.

I. BACKGROUND AND INTRODUCTION

Mass accommodation coefficient (MAC) is a key parameter determining mass flow at the liquid-vapor interface and the rate of the heat exchange due to evaporation/condensation processes. Fundamentally, MAC is defined as the fraction of vapor molecules that upon collision with the liquid are "adsorbed (accommodated)" rather than reflected (not accommodated). MAC provides microscopic bases for the kinetic theory of evaporation. In particular, kinetic theory of gases as well as thermodynamic considerations lead to a description of the net evaporative molecular flux at the evaporating liquid-vapor interface given by the Hertz-Knudsen[1] relation

$$J_{\mathrm{m}} = \frac{1}{\sqrt{2\pi m k_B}}\left(\sigma_e \frac{P_{\mathrm{eq}}(T_{\mathrm{L}})}{\sqrt{T_{\mathrm{L}}}} - \sigma_c \frac{P_{\mathrm{v}}}{\sqrt{T_V}}\right), \tag{1}$$

where σ_{e} (evaporation coefficient) and σ_{c} (condensation coefficient) are kinetic factors which were introduced as separate coefficients to achieve better description of experimental observations.[2] The difference in the saturated vapor pressure at the liquid temperature, $P_{\mathrm{eq}}(T_{\mathrm{L}})$, and the vapor pressure P_{v} is the thermodynamic driving force for condensation or evaporation. σ_{c} is also known as the mass accommodation coefficient (α) and is often assumed to be equal to the σ_{e},[2,3] as they have to be equal to each other in equilibrium. α is used as a fitting parameter in the analysis of experimental data due to the difficulty in accurate determination of this coefficient, as well as thermodynamic conditions at the interfaces.[2] Knowledge of the molecular flux can be used to evaluate the thermal energy flux by multiplying J_{m} by the molecular enthalpy of evaporation. Also, Eq. (1) shows that in systems not far away from equilibrium, the local vapor pressure near the liquid-vapor interface is essentially equal to the saturation pressure—such an assumption is made for initial stages of the collapsing vapor bubbles.

In the Hertz-Knudsen treatment of evaporation, the molecular velocity distribution in the vapor near an interface is assumed to be unaffected by the evaporation flux. Schrage's analysis[4,5] showed that the drift velocity of molecules in the vapor near the interface has the effect of increasing the effective evaporation coefficient (equal to the effective condensation coefficient), and it introduced an additional factor of

$$\eta = \frac{2\alpha}{2-\alpha} \tag{2}$$

in the Hertz-Knudsen relation in the limit of small driving forces. In the limit of perfect mass accommodation, i.e., $\alpha = 1$, Schrage's derivation yields $\eta = 2$. Our molecular dynamics simulation results

on a steady state evaporation-condensation system indicate that Hertz-Knudsen-Schrage equation describes the observed flux very well in the limit of small driving forces and that exact Schrage analysis is accurate over a wide range of conditions.[6]

Despite these long-term efforts, quantification of MAC remains challenging experimentally. For example, analysis of experiments of droplet condensation yielded a wide range of α from 0.04 to 1.00.[7] Some prior studies of α have focused on evaporation of liquid confined in micro-capillaries where other limitations on mass transport can be minimized.[8–11] Also, Lee *et al.* studied transport of water through hydrophobic nanopores and found a condensation probability on the order of 0.3.[12] Accurate modeling of such experiments, however, is challenging because of the curvature of the liquid interface and its relatively complex geometry.

From the modeling side, in molecular dynamics (MD) simulations where MAC is determined directly from observations of trajectories of atoms/molecules impacting the liquid from the vapor phase, the mass accommodation coefficients for water and model Lennard-Jones (LJ) fluids are consistently close to unity.[13–16] This finding is in stark contradiction with values of MAC $\ll 1$ that have been invoked to explain specific experiments. A large range of MAC deduced from experiments can be due to several factors, such as experimental measurement accuracy, the influence of extrinsic conditions, and the fact that the actual measurements are not directly of MAC but of phenomena affected by MAC, such as the rate of growth of droplets embedded in supersaturated vapor. Another uncertainty is the estimation of the vapor and liquid temperature/pressure conditions near the interface that is very challenging experimentally.

The situation is even more challenging in the case of collapsing vapor bubbles where the system is highly dynamic and can be far away from equilibrium. In the case of cavitation dynamics, vapor bubbles, generated by, e.g., sonication, collapse and generate a high temperature and pressure environment often leading to the generation of light.[17] One of the key aspects in predicting the temperature/pressure condition during the droplet collapse is the MAC. In many models, it is assumed that up to some critical radius (or velocity that can reach values of several km/s) of the liquid-vapor interfaces of the collapsing bubble, the vapor is in local equilibrium with the liquid and the pressure does not increase, as the vapor simply condenses on the liquid. At higher velocities, it is assumed that the condensation rate is insufficient to maintain local equilibrium and the collapsing bubble compresses the vapor.[18,19] In applications such as spray cooling, microdroplets of coolants impinge on a heated surface and form a thin liquid film, which then evaporates and removes heat efficiently from the material.[20,21] Although the velocity of impingement is not km/s[20,22] in these applications, there could be some deviation in the MACs as compared to stationary interfaces for other coolants. Lin and Ponnappan[23] showed that the presence of non-condensable gases in spray cooling chambers alters the thermal performance of the system. Thus, variation in MAC with the speed of moving interface could potentially affect the spray characteristics and consequently the cooling process.

To explore the molecular origin of these assumptions and to quantify the potential transition from accommodating to non-accommodating vapor, we will perform MD simulations allowing for determination of the mass accommodation coefficient directly from the molecular trajectories and investigate its dependence on the liquid-vapor interface velocity.

The rest of this article is organized as follows: In Sec. II, we will describe molecular dynamics simulations of MAC as a function of the velocity of the liquid-vapor interface for an atomic-level model of water. In Sec. III, we will present the effects of parameters and collision rules determined in water simulations on the pressure, temperature, and density of vapor subjected to a high-velocity liquid-vapor interface. Finally, we will present a summary and conclusions in Sec. IV.

II. MOLECULAR DYNAMICS SIMULATIONS OF WATER MASS ACCOMMODATION

To determine MAC at the liquid-vapor interface, we use molecular dynamics simulations where we can monitor individual vapor molecule—liquid water collision events. Such simulations allow for a direct determination of MAC from its microscopic definition and enable us to gain deeper insight into the collision process. Furthermore, information and parameters obtained in these simulations will be used in simplified model studies on the high-velocity liquid sweeping its own vapor, which is relevant to the phenomenon of collapsing vapor bubbles (see Sec. III).

A. Model and simulation method

The TIP4P-Ew water model[24] was used in the present simulations. This model of molecular water is capable of good representation of the liquid and vapor phases and their coexistence. It has been used to reproduce surface tension over a wide range of temperatures, with the boiling point and critical temperature being within ~5% of the experimental values,[25] and was successfully used to simulate water liquid/vapor systems at patterned gold surfaces.[26] To achieve computational efficiency, Coulombic interactions were calculated using the particle-particle particle-mesh (PPPM) method[27] and the intramolecular bonds were constrained using the SHAKE algorithm.[28] The MD simulations were performed using the LAMMPS package[29] with a time step of 1 fs which was proved to be sufficient to simulate the motion of water molecules.

The initial configuration consisted of a liquid slab with a thickness of about 30 Å in the center of the simulation cell and the vacuum space at both sides of the slab. The snapshot of one half of a simulation cell is shown in Fig. 1. The vacuum-liquid interfaces were perpendicular to the z-direction, and the periodic boundary conditions were used in all directions. The linear dimension of the simulation cell in the z-direction was fixed at 124 Å, while to assess possible fine size effects, we varied the linear dimension L parallel to the interface from 15 to 155 Å, resulting in 250–25 000 water molecules in the liquid slab.

The system was first equilibrated at 300 K for 50 ps at a constant volume and temperature (NVT ensemble) using a Nose-Hoover thermostat. In the next step, one by one, individual vapor phase water molecules were injected into the system at 10 ps intervals and destined to collide alternatively with the top and the bottom liquid-vapor interfaces. The insertions were done at a distance of 15 Å from the liquid-vapor interfaces at random x and y coordinates. The velocities of the incident molecules were selected from the half Maxwell-Boltzmann velocity distribution at 300 K, where the z

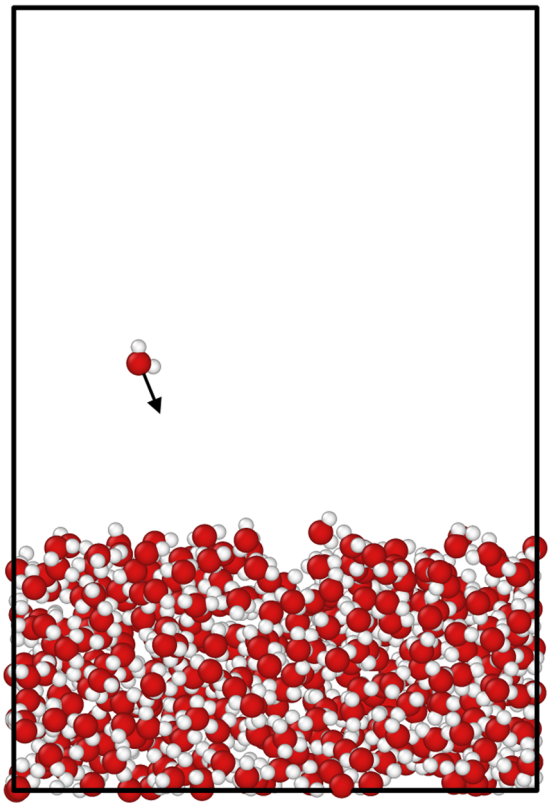

FIG. 1. Schematic figure illustrating the top half of the simulation system. The vacuum-liquid interface is perpendicular to the z-direction. Vapor phase water molecules are injected 15 Å above the liquid-vapor interface with a velocity selected from the Maxwell distribution with an additional normal to interface velocity mimicking the process of a collapsing water vapor bubble.

component of the velocity was always pointing to the interface.[13] Furthermore, a normal-to-the-interface velocity component, V_{add}, was added to the thermal velocity to mimic a high velocity collapsing vapor bubble.

Ten incident molecules were generated in a single simulation run, and we performed 300 independent simulation runs for each value of v_{add} (ranging from 0 to 10 km/s) and each system size to assure good statistics and to assess the statistical errors. The injected molecules were not subject to the thermostat action, or temperature calculations to avoid the effects of their high kinetic energy, while the liquid slab molecules were continuously thermostated to mimic thermal coupling with a large liquid reservoir.

We determined MAC simply by counting the fraction of incident gas phase water molecules that were accommodated by the liquid. The count was done automatically by monitoring ejected/reflected molecules passing the virtual planes at a distance of 35 Å from the liquid-vapor interface. The leaving time and positions of the molecules departing from the interface were calculated and compared to the injected molecules to distinguish the ejection and evaporation events. In several cases, we performed count of ejection events by visual inspection of molecular trajectories to verify that our automatic count procedure is accurate.

It is well known that the liquid-vapor interface exhibits thermodynamic fluctuations with temperature and lateral size dependent interfacial width. This might affect the value of the MAC. Therefore, we simulated systems with a range of lateral sizes and obtained the density profiles as shown in Fig. 2(a). Using such profiles determined, the width, w, of the liquid-vapor interface w was from the fitting parameters for the hyperbolic tangent function

$$\rho = \frac{\rho_0}{2}\left[\tanh\left(\frac{z - z_0}{w}\right) + 1\right], \tag{3}$$

where ρ is the density, ρ_0 is bulk liquid density, z is the coordinate along normal to the interface direction, and z_0 is the location of the interface.

The analysis of the interfacial fluctuations[30,31] suggests a logarithmic increase in the interfacial width w with increasing lateral dimension L. Indeed, as shown in Fig. 2(b), the interfaces simulated by us exhibit such a scaling. In the context of the MAC determination, we note that the interfacial width, even for the largest system size studied, is of the order of 2 Å, which is much smaller than other relevant dimensions, such as potions of the plane where vapor molecules are injected, or a plane where ejected molecules are identified.

B. Results and discussion

In the majority of the collision events, when the incident water molecule reached the liquid surface, it was accommodated. Another outcome was the reflection of the incoming molecule, sometimes accompanied with an ejection of other molecules. For the purpose of simplicity, we will call all not fully accommodating events as ejection events. Using this terminology, the ejected molecules can be either the reflected incident molecules or other molecules ejected from the liquid due to the collision. There may be more than one ejected molecule in a collision event, leading to a number of ejected molecules larger than the number of ejection events. However, in the vast majority of the cases, there was either none or only one ejected molecule.

All MACs were evaluated at 300 K at several values of the V_{add}. The resulting MAC as a function of interfacial lateral size, L, is shown in Fig. 3(a). When V_{add} = 0, we determine the mass accommodation coefficient to be about 0.99, i.e., essentially unity, and essentially independent from L. Such a value is consistent with

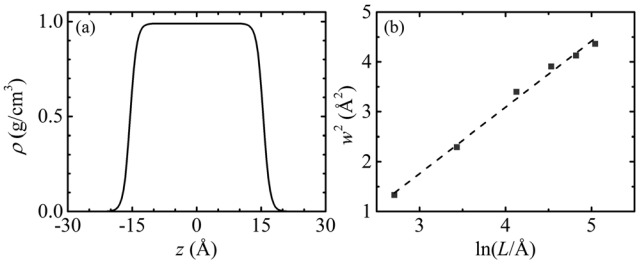

FIG. 2. (a) Density profile of the equilibrated liquid water slab along the z direction. (b) The logarithmic finite-size dependence of the interfacial width w on the lateral dimension L of the interface. Red squares are the data points, and the dashed line is a linear fitting curve.

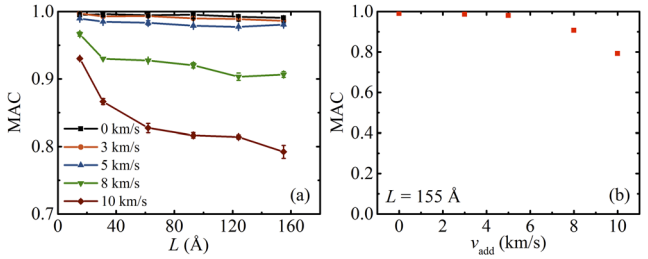

FIG. 3. (a) The mass accommodation coefficient of water at 300 K as a function of the lateral dimension of the interface with different macroscopic liquid-vapor interface velocity v_{add}. (b) The mass accommodation coefficient of water at 300 K as a function of v_{add} when L = 155 Å.

previous MD studies of water at room temperature using the TIP4P-Ew water model,[16] the SPC/E water model[13,14] and the POL3 water model.[15]

With increasing V_{add}, MAC gradually decreases. Interestingly for V_{add} = 8 and 10 km/s, the value of MAC first decreases significantly with increasing system size; however, it appears so saturate for larger system sizes. It is also interesting that even for the highest velocity of and at V_{add} = 10 km/s, the value of the MAC is still very high and equal to about 0.80 [see Fig. 3(b)]. For this high V_{add}, the associated kinetic energy is about 200 times larger than the average thermal kinetic energy at 300 K and 20 times larger than the water heat of vaporization. This result indicates that the assumptions made about the lack of accommodation at high collapse velocities in continuum modeling of collapsing vapor bubbles cannot be justified by the intrinsic water liquid-vapor interfacial properties.

To get deeper insight into the collision process, particularly, involving ejection events, we analyzed the velocities of all ejected molecules in the case of V_{add} = 10 km/s. The data on velocity distributions, based on statistics obtained from a total of about 400 ejection events, are presented in Fig. 3. As demonstrated in Figs. 4(a) and 4(c), velocity components parallel to the liquid-vapor interface and speed distributions can be well fitted to the Maxwell-Boltzmann distribution at a single temperature of 3300 K. We also plotted the normal to the interface velocity distribution—along with $\frac{1}{2}$ of the Boltzmann distribution (at 3300 K), as in this case, all ejected atoms move in one direction away from the interface. The fit is good at a large velocity range, but it deviates from the data in the small velocity range. We do not know what the origin of these relatively good fits is. These good fits are particularly puzzling since the ejection events represent highly non-equilibrium process, while the Maxwell-Boltzmann distribution is an equilibrium characteristic.

The temperature of 3300 K corresponds to the average thermal velocity of about 2.15 km/s. Considering that the impact velocity was ≈10 km/s, we estimate that at these conditions, in case of the ejection event, about 4.5% of the kinetic energy of the incoming molecules is converted into the kinetic energy of the ejected molecules, while the remaining energy is "accommodated" by the liquid. Of course, during accommodation events, all incoming energy is accommodated.

These observations are not limited to the V_{add} = 10 km/s case. According to Fig. 5, the average kinetic energy of ejected molecules increases linearly as a function of kinetic energy of

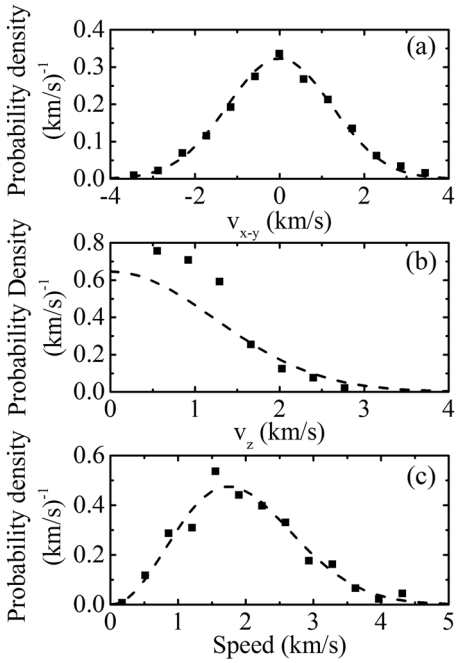

FIG. 4. The distributions of the velocity components and speed of ejected molecules for V_{add} = 10 km/s. The black squares are data, and the dashed lines represent the Maxwell-Boltzmann distributions at 3300 K.

incoming molecules. The slope of the linear fit is ~0.04, and the vertical axis intercept (at V_{add} = 0) is about 0.5 $(km/s)^2$. The square root of the intercept is equal to 700 m/s which is close to the root mean square speed of water at T = 300 K, which has a value of 644 m/s. The understanding of the value of the slope is not that straightforward, as the slope represents the kinetic energy fraction of the incoming molecules converted into the kinetic energy of the ejected molecules. This fraction represents a result of a complex process of

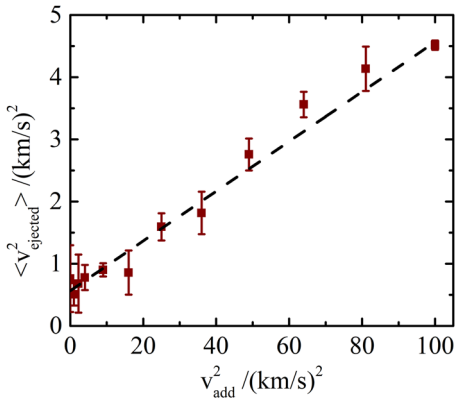

FIG. 5. Relation between the mean square speeds of ejected molecules and the square of V_{add}. The dashed line is the fitting line with a slope of 0.04. The intercept with the vertical axis is 0.5 $(km/s)^2$.

molecular collisions with a liquid, i.e., viscoelastic medium with molecular structure.

However, the slope in Fig. 5 can be related to the translation thermal (or energy) accommodation coefficient (TAC) of water vapor molecules on liquid water surfaces. TAC is defined as[32]

$$\frac{E_r - E_i}{E_s - E_i}, \tag{4}$$

where E_i and E_r are the kinetic energy of incident and reflected/ejected molecules and E_s is the average energy of molecules in thermal equilibrium with the liquid surface. Since in our simulations E_i is typically much greater than E_s, TAC is approximately equal to $1 - E_r/E_i$. According to Fig. 5, $E_r/E_i = 0.04$, thus TAC is approximately equal to 0.96. This is only semi-quantitative analysis as the evaluation of TAC should also account for molecules that are "mass accommodated" to the liquid, while data in Fig. 5 only account for the kinetic energy of molecules that are not accommodated. Furthermore, within the scope of this paper, we only consider translational kinetic energy and associated TAC, while there is also rotational TAC characterizing rotational kinetic energy transfer. Nevertheless, the large, close to unity, value of TAC is consistent with observations of large TAC when gas molecules collide with soft surfaces.[33]

III. MOLECULAR SIMULATIONS OF THE VAPOR SUBJECTED TO A RAPIDLY MOVING LIQUID VAPOR INTERFACE

As we discussed in the Introduction, a key motivation of our work was to relate to the studies of vapor bubbles collapsing at high velocities (~several km/s). We envision that the results presented above can be used in the continuum-scale modeling of the process that can be directly connected to the experimental time and length scales. To illustrate the effect of the MAC on the vapor inside the collapsing bubble, we performed a set of molecular dynamics simulations on a simplified vapor model. In these simulations, the liquid is mimicked by an imaginary moving interface with which the vapor molecules collide according to the rules determined by the explicit water model simulations described in Sec. II. The vapor is represented by monoatomic gas. Furthermore, we make additional simplifying assumptions, such as constant temperature of the liquid at the liquid-vapor interface. Consequently, this model should be considered as a kinetic collision solver for a general problem of rapidly moving liquid-vapor interface, rather than a model of water liquid-vapor moving interface.

A. Model and simulation methodology

The snapshot of the simulation cell is shown in the top panel of Fig. 6. The simulation cell has a cross section of 5 nm × 5 nm and a length (along the z direction) of 200 nm. Periodic boundary conditions are applied in the x and y directions. On the right-hand edge of the cell, a fixed, impermeable wall was introduced, which had repulsive harmonic interactions with the vapor atoms. Initially, an analogous wall was placed on the left-hand edge of the simulation cell.

In this simplified model, molecules were represented by atoms interacting through Lennard-Jones (LJ) potentials with parameters representing argon.[6] We used a shifted force LJ potential with an interaction cutoff radius of 3.82 Å to consider only repulsive interactions and avoid any possibility of phase change. Consequently, atoms in our model represent soft repulsive spheres. The simulation cell contained a total of 2000 atoms and was first equilibrated at 300 K for 10 ps using the Nose Hoover thermostat with a simulation time step of 1 fs. Under these conditions, the resulting pressure was about 17 atm. The use of this relatively large pressure was motivated by our desire to have the simulation cell length significantly larger than the molecular collision mean free path. Under such conditions, a connection with macroscopic description of the system can be made. We estimated the mean free path to be about 5 nm, making the initial length of the simulation cell approximately 20 times larger.

After equilibration, the left-side wall was used to mimic the moving liquid vapor interface. We accounted for processes simultaneously occurring at this interface: (i) equilibrium evaporation of liquid at 300 K, (ii) ejection due to vapor molecules collisions with the liquid, and (iii) accommodation of the vapor molecules colliding with the liquid.

The evaporation rate was evaluated by calculating the rate of incoming vapor molecules in equilibrium (stationary wall). Since, for water at 300 K, the MAC is essentially equal to unity, the rate of incoming vapor molecules should be equal to the rate of evaporating atoms to maintain equilibrium. In the simulations with the moving wall representing the liquid-vapor interface, to model evaporation, we inserted molecules at the fixed equilibrium rate calculated for the stationary wall with velocities sampled from the Maxwell-Boltzmann velocity distribution at 300 K and added the moving wall velocity, V_{add}, to the z component of these velocities.

To explore the role of assumptions made about the value of the MAC, we considered 3 cases represented by a corresponding collision rule. (a) Full accommodation (MAC = 1): atoms were eliminated from the simulation cell upon collision with the wall. (b) No accommodation (MAC = 0): atoms were re-injected to the simulation cell with a random velocity taken form the Maxwell-Boltzmann distribution at T = 3300 K (see Sec. II) plus V_{add} in the z direction. (c) Partial accommodation (MAC = 0.80): this corresponds to the values obtained from explicit simulations of water for V_{add} = 10 km/s (see Sec. II). Here with a probability of 80%, atoms were eliminated from the simulation cell upon collision with the moving wall, and with 20% probability, they followed non-accommodation rules described in (b). In all simulated cases, the moving wall velocity was V_{add} = 10 km/s, and 5 independent runs were performed for each of (a)–(c) cases.

B. Results and discussion

Figure 6 shows variations in number density, temperature, and pressure as a function of time when the left-side wall moves with a high velocity of 10 km/s. When MAC = 0, the wall mimics an impenetrable piston. In this case, the density, pressure, and temperature increase at the fastest rate; as upon collision, the vapor atoms are always injected back into the vapor phase with high velocities. The other extreme case, MAC = 1, characterizes a surface which absorbs every atom that crosses it. In this case, there is a slight increase in temperature associated with high velocity of the evaporated atoms. As the temperature in the vapor increases, the rate of atoms colliding

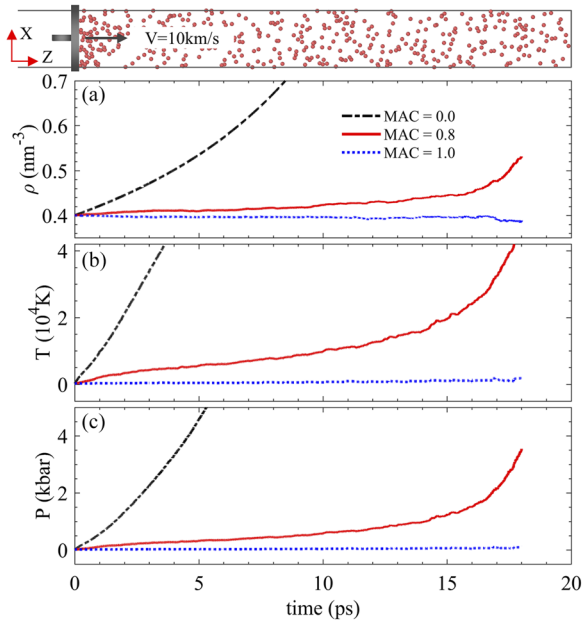

FIG. 6. Top panel: Snapshot of atomic positions of vapor atoms subjected to 10 km/s "piston" mimicking a moving liquid-vapor interface. (a) The number density, (b) temperature, and (c) pressure of the vapor as a function of time. Dashed-dotted line: non-accommodating interface (MAC = 0); solid line: interface with MAC = 0.87; dashed line: fully accommodating interface (MAC = 1).

with the moving wall also increases, and thus, the number density decreases since we use a constant evaporation rate obtained from equilibrium simulations at 300 K.

The case of MAC = 0.80 corresponds to the value obtained for molecular water at a liquid-vapor interface moving with 10 km/s velocity. This scenario corresponds to a high-velocity collapsing vapor bubble, with the bubble containing only water vapor molecules (i.e., no other gases). Although 20% of the atoms are not accommodated, the density buildup is not very significant and much smaller than that characterizing a non-accommodating wall. The pressure and temperature increase significantly here due the high velocity injected atoms; however, the corresponding increases are far smaller than in the case of a non-accommodating wall.

While the simulation model and conditions described in this section are highly simplified, the actual collapse of the vapor bubble, the dramatic differences between the MAC = 0.80 case, and the non-accommodating case suggests that the assumptions about the lack of vapor accommodation beyond some critical collapsing bubble radius (or velocity) cannot be attributed to intrinsic properties of pure water liquid-vapor interfaces. We might speculate that in the case of real collapsing bubbles, impurities, such as non-soluble organic molecules, accumulate at the liquid-vapor interfaces. With a sufficiently large surface density of such impurities, water vapor accommodation can be suppressed. Further complexity of the real bubble collapse comes from the presence of non-condensable gases, such as oxygen and nitrogen, which will inevitably affect the pressure and temperature density variations. Furthermore, during the actual collapse, the liquid near the interface becomes warmer and shock waves can be present. All these effects are not accounted for our model.

IV. SUMMARY AND CONCLUSIONS

We used molecular dynamics simulation to determine MAC as a function of the velocity of the liquid-vapor interface for the atomic-level model of water. We found that even at very high interfacial velocity, over an order of magnitude higher than average thermal molecular velocity, MAC is only moderately smaller than unity. Analysis of those molecules that get reflected or ejected from the interface indicates that a high fraction of impact energy is adsorbed during the collision process.

Using the parameters and collision rules determined in water simulations, we performed atomistic simulations of a simple vapor model and determined pressure, temperature, and density buildup at the front of the high-velocity, liquid-vapor interface. Interestingly, due to a high MAC, there is almost no density buildup, which contrasts with the situation where MAC is small. There is a temperature and pressure buildup due to the injection of high-kinetic energy molecules to the vapor.

Our results have implications for continuum-level modeling of collapsing vapor bubbles. In such continuum models, an assumption is made that during the collapse, the interface is accommodating (or near local thermodynamic equilibrium) and later becomes non-accommodating. The fact that our simulations show a high degree of accommodation even for very high-velocity interfaces suggests that the transition from an accommodating to non-accommodating liquid-vapor interface is not an intrinsic property of pure water. We speculate that the origin of this transition is associated with impurities, such as non-soluble molecules that accumulate at the interface and at a vapor bubble radius small enough to accommodate them, which would provide high interfacial coverage, thus obstructing water condensation-evaporation processes.

ACKNOWLEDGMENTS

This work was supported by the Office of Naval Research Thermal Science Program, Award No. N00014-17-1-2767. This work was also supported by the New York State NYSTAR funded Focus Interconnect Center.

REFERENCES

[1]M. Knudsen, *The Kinetic Theory of Gases: Some Modern Aspects* (Methuen & Company Limited, Methuen, 1934).
[2]R. Marek and J. Straub, Int. J. Heat Mass Transfer **44**, 39 (2001).
[3]R. Hołyst, M. Litniewski, D. Jakubczyk, K. Kolwas, M. Kolwas, K. Kowalski, S. Migacz, S. Palesa, and M. Zientara, Rep. Prog. Phys. **76**, 034601 (2013).
[4]J. Barrett and C. Clement, J. Colloid Interface Sci. **150**, 352 (1992).
[5]R. W. Schrage, *A Theoretical Study of Interphase Mass Transfer* (Columbia University Press, New York, 1953).
[6]Z. Liang, T. Biben, and P. Keblinski, Int. J. Heat Mass Transfer **114**, 105 (2017).
[7]A. Laaksonen, T. Vasala, M. Kulmala, P. M. Winker, and P. E. Wagner, Atmos. Chem. Phys. **5**, 461 (2005), and references therein.
[8]H. Wang, S. V. Garimella, and J. Y. Murthy, Int. J. Heat Mass Transfer **50**, 3933 (2007).
[9]S. Narayanan, A. G. Fedorov, and Y. K. Joshi, Langmuir **27**, 10666 (2011).
[10]C. Duan, R. Karnik, M.-C. Lu, and A. Majumdar, Proc. Natl. Acad. Sci. U. S. A. **109**, 3688 (2012).

[11] A. A. Avdeev and Y. B. Zudin, High Temp. **50**, 527 (2012).
[12] J. Lee, T. Laoui, and R. Karnik, Nat. Nanotechnol. **9**, 317 (2014).
[13] A. Morita, M. Sugiyama, H. Kameda, S. Koda, and D. R. Hanson, J. Phys. Chem. B **108**, 9111 (2004).
[14] T. Tsuruta and G. Nagayama, J. Phys. Chem. B **108**, 1736 (2004).
[15] J. Vieceli, M. Roeselová, and D. J. Tobias, Chem. Phys. Lett. **393**, 249 (2004).
[16] J. Julin, M. Shiraiwa, R. E. H. Miles, J. P. Reid, U. Pöschl, and I. Riipinen, J. Phys. Chem. A **117**, 410 (2013).
[17] S. J. Putterman and K. R. Weninger, Annu. Rev. Fluid. Mech. **32**, 445 (2000).
[18] M. C. Ramsey and R. W. Pitz, Phys. Rev. Lett. **110**, 154301 (2013).
[19] M. C. Ramsey, "Energetic cavitation collapse," Ph.D. thesis, Vanderbilt University, 2013.
[20] S. G. Kandlikar and A. V. Bapat, Heat Transfer Eng. **28**, 911 (2007).
[21] J. Kim, Int. J. Heat Fluid Flow **28**, 753 (2007).
[22] H. Montazeri, B. Blocken, and J. Hensen, Build. Environ. **83**, 129 (2015).
[23] L. Lin and R. Ponnappan, Int. J. Heat Mass Transfer **46**, 3737 (2003).
[24] H. W. Horn, W. C. Swope, J. W. Pitera, J. D. Madura, T. J. Dick, G. L. Hura, and T. Head-Gordon, J. Chem. Phys. **120**, 9665 (2004).
[25] R. Sakamaki, A. K. Sum, T. Narumi, and K. Yasuoka, J. Chem. Phys. **134**, 124708 (2011).
[26] H. Hu, C. R. Weinberger, and Y. Sun, Nano Lett. **14**, 7131 (2014).
[27] R. W. Hockney and J. W. Eastwood, *Computer Simulation Using Particles* (Hilger, Bristol, 1989).
[28] J. P. Ryckaert, G. Ciccotti, and H. J. C. Berendsen, J. Comput. Phys. **23**, 327 (1977).
[29] S. Plimpton, J. Comput. Phys. **117**, 1 (1995).
[30] S. W. Sides, G. S. Grest, and M. D. Lacasse, Phys. Rev. E **60**, 6708 (1999).
[31] F. Schmitz, P. Virnau, and K. Binder, Phys. Rev. E **90**, 012128 (2014).
[32] S. C. Saxena and R. K. Joshi, *Thermal Accommodation and Adsorption Coefficients of Gases* (Hemisphere Publishing Corporation, New York, 1989).
[33] Z. Liang, W. Evans, T. Desai, and P. Keblinski, Appl. Phys. Lett. **102**, 061907 (2013).